Automated Marangoni Monolayer Technique: Design Review

MEIE 4702: Capstone 2

Team Members

Nolan Donohue

Brooke Kotopoulos

Cory Lafleur

Jonathan Tansey

Alexander Zeng

Team Advisor

Prof. Randall Erb

December 12th, 2022

Department of Mechanical and Industrial Engineering

College of Engineering, Northeastern University

Boston, MA 02115

Automated Marangoni Monolayer Technique: Design Review

Nolan Donohue, Brooke Kotopoulos, Cory Lafleur, Jonathan Tansey, Alexander Zeng

Abstract

Percolated hexagonal boron nitride (hBN) monolayers have attracted attention from industry to be used for applications which require coatings that dissipate heat without interfering with radio frequencies, such as radomes. A manual, small-scale procedure, which used the Marangoni effect to densify a Langmuir film, has proven successful at manufacturing these monolayers, but its efficacy at industrial scales has yet to be explored. Thus, the goal of this project was to provide a solution that precisely automated the reliable creation of large-scale, percolated hBN monolayers. The design was subdivided into three subsystems: sample injection, Marangoni densification, and monolayer transfer. Each subsystem was independently researched, designed, and validated such that, when combined, these three subsystems would produce a monolayer on a solid substrate. Adjustability and simplicity were at the core of the design of each subsystem to allow for rapid iteration and rigorous testing. The final large-scale design integrated the three subsystems with a sturdy frame and an intuitive user interface. Testing proved that the large-scale prototype was successful at fully coating a 9in-by-9in PVC substrate with an hBN monolayer. The prototype is expected to be used in Northeastern's Directed Assembly of Particles and Suspensions laboratory to assist researchers in developing monolayers with optimal thermal and electrical properties.

Table of Contents

List of Figures

List of Tables

1 Introduction

As electronics continue to become more powerful, their heat dissipation requirements increase. Traditional metal heat sinks cannot be used in applications which involve incoming and outgoing radio frequencies (RF) as metal obstructs the RF signals. An example problematic application of metal heat sinks is radomes, the protective covering around a radar. Radomes must effectively dissipate heat from the radar's electronics while not interfering with RF. Therefore, non-metallic materials were explored to find ones that had high thermal conductivities while being transmissible to RF. A particularly interesting material to meet those goals was percolated hexagonal boron nitride (hBN) monolayers. Hexagonal boron nitride monolayers have thermal conductivities of up to 20 W/m·K, which is competitive compared to other photonic crystal-based heat sinks [1]. Additionally, the extremely thin monolayers, only a single layer of particles thick, cause little to no interference of RF. Consequently, hBN monolayers have attracted the attention of industry for radome applications. Figure 1 below is a graphical depiction of the advantageous thermal and electrical properties of percolated monolayers of hBN when applied to radomes.

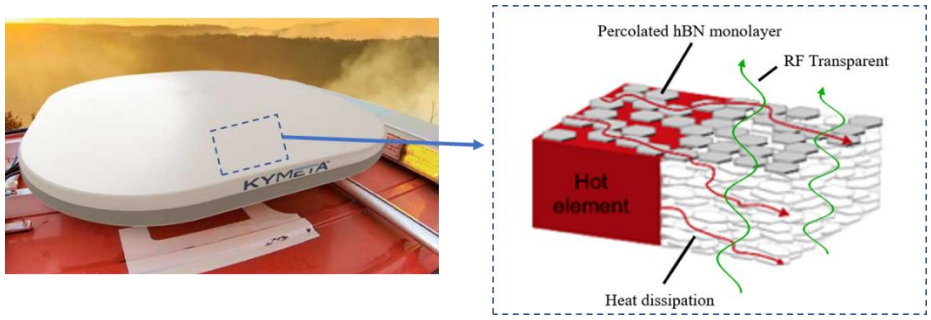

Figure 1: Image of radome with a diagram of percolated hBN monolayers

A process for manufacturing hBN monolayers has been developed by researchers at Northeastern's Directed Assembly of Particles and Suspensions (DAPS) laboratory. However, this process has only been completed manually on a small-scale, producing 3in-by-1in monolayers. Manually creating monolayers with the dimensions required for industrial applications is extremely time-consuming and challenging. Therefore, to manufacture large-scale monolayers, this process must be automated. Automation both reduces human error and increases the throughput of the process. Manual steps will still be required before and after the process for setup and post-processing. A successful device is one that can reliably coat a 9in-by-9in solid substrate with highly dense hBN monolayer.

2 Background Review

The goal of the background review was to understand the current process used to create monolayers at demo-scale, the underlying physics behind each subsystem to be able to identify and mitigate risks, and the current commercial offerings to know what features are required to make a product competitive on the market. The current demo-scale process was observed at Northeastern's DAPS Laboratory. Three subsystems were identified: injection, Marangoni, and transfer. From there, research was conducted to understand the physical phenomena occurring to identify risks of each subsystem and what had to be done to mitigate those risks. The identified risks of the injection, Marangoni, and transfer subsystems were sedimentation, parallelism, and material selection, respectively. A review of current commercial offerings highlighted the need for fine control and automatic sample injection while showing a gap in the market for large-scale monolayer manufacturing techniques that this project could satisfy.

2.1 Process Overview

The goal of this Capstone project is to coat a 9in-by-9in solid substrate in a homogenous and densified monolayer of hBN. The process to create this monolayer has been proven at a demo-scale with a fully manual technique by researchers in Northeastern's DAPS Laboratory [2]. The lab's current, small-scale process consists of three steps: sample injection, Marangoni densification, and monolayer transfer.

To begin, a solution of ethanol and hBN particles are injected onto an air-water interface of a trough containing deionized water. Once a desired concentration of hBN particles is suspended on the interface, a drop of soap is added to one side to induce the Marangoni effect. The soap causes the particles to densify toward the opposite side of the trough. Lastly, the monolayer is transferred off the air-water interface onto a solid substrate. The current transfer procedure involves sliding a substrate beneath the water and gently pulling it up through the monolayer at an angle. Figure 2 on the next page shows the three steps used to create a monolayer.

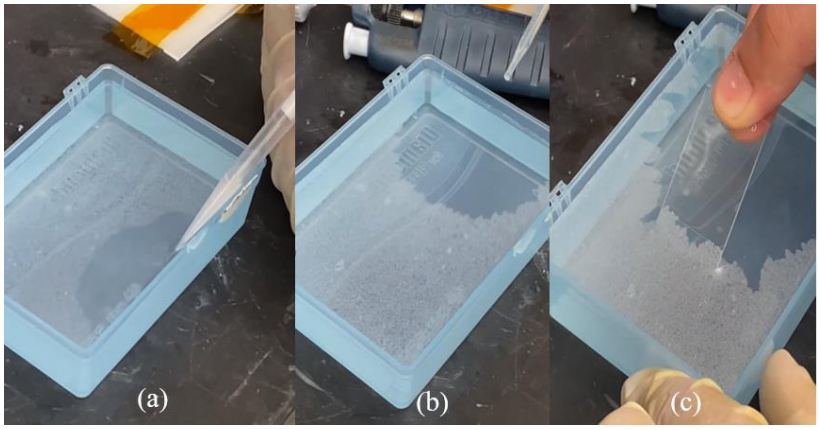

Figure 2: Demo-scale procedure of a) sample injection, b) Marangoni densification, and c) monolayer transfer [2]

The limitations of the current demo-scale process are repeatability and scalability. The fully manual nature of the current process introduces a lot of variability between trials and therefore it is difficult to achieve a highly densified monolayer. In addition, the throughput of this process is low as it depends on a human operator. The process must be automated to both scale the process and increase the throughput. Therefore, the goal of this Capstone team is to semi-automate and scale up this process so that a single run will reliably result in a fully coated 9in-by-9in substrate in a dense monolayer.

There are three determined subsystems, like the three steps of the manual process, which must be automated: injection, Marangoni, and transfer. The first subsystem, injection, must mix hBN and ethanol and add the partiscles onto the air-water interface of the trough. The second subsystem is the Marangoni subsystem which must be capable of adding soap into the trough to cause particle densification. The final subsystem, transfer, must transfer a large enough section of the particle monolayer to fully coat a 9in-by-9in solid substrate. In addition to these three automated subsystems, a frame that encompasses the entire system and all necessary software and electronics must be designed by the team.

2.2 Principals and Concepts

A basic understanding of the fundamental physics of each of the required subsystems is important to inform design decisions and identify potential risks. Presented in this section is a rudimentary explanation of the various physical phenomena that are important for the process. First, an introductory section on the concepts of surface tension and wettability details an underlying concept that is important to all subsystems. Then, the specific principles involved in each individual subsystem will be explained in their own sections.

2.2.1 Surface Tension and Wettability

Surface tension is a property of liquids that describes the net force acting on a liquid surface that causes it to act like an elastic membrane [3]. The difference in cohesive forces between the bulk and surface of a liquid give rise to the surface tension [4]. While numerical values for the surface tension of various liquids can be obtained, they are not important for the purposes of this Capstone project. Instead, a comparison of the surface tensions between two fluids is important to note as will be explained in the discussion of the Marangoni effect. The liquids relevant to this Capstone project are water and sodium lauryl sulfate (soap). Soap has a lower surface tension than water [2].

Surface energy is equivalent to surface tension, but for solids instead of liquids. Surface energy is the attractive force between molecules at the surface of a solid [5]. When liquids and solids are brought into contact with each other, the concept of wettability can be defined based on a balance of the surface tension of the liquid, the surface energy of the solid, and the adhesive forces between the liquid and solid [6]. A formal definition of wettability is the ability of a liquid to remain in contact with a solid surface [7]. Figure 3 below shows an example of a wetting and non-wetting surface.

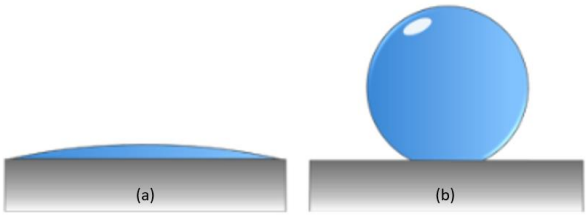

Figure 3: Diagram of a) wetting surface and b) non-wetting surface [7]

The wetting surface shown in panel a) enables the liquid to spread out upon the solid surface. The surface energy of the solid is strong compared to the surface tension of the liquid enabling the surface to pull the liquid droplet down. Alternatively, the non-wetting surface in panel b) causes the liquid to remain in almost a spherical shape rather than spreading out across the surface. The surface tension of the liquid is stronger than the surface energy of the solid so the liquid stays clumped together [8].

A common way to measure the wettability of a substance is through the contact angle. The contact angle is defined as the angle that the liquid makes with a solid surface [9]. A contact angle of less than 90° is commonly defined as wettable, and a contact angle greater than 90° is called non-wettable. Figure 4 on the next page depicts how the contact angle is measured for a wettable and non-wettable surface. When water is used as the measuring liquid, a wettable surface is called hydrophilic, and a non-wettable surface is called hydrophobic [6]. A contact angle goniometer is used to image water droplets upon a solid surface and enables the contact angle to be measured [10].

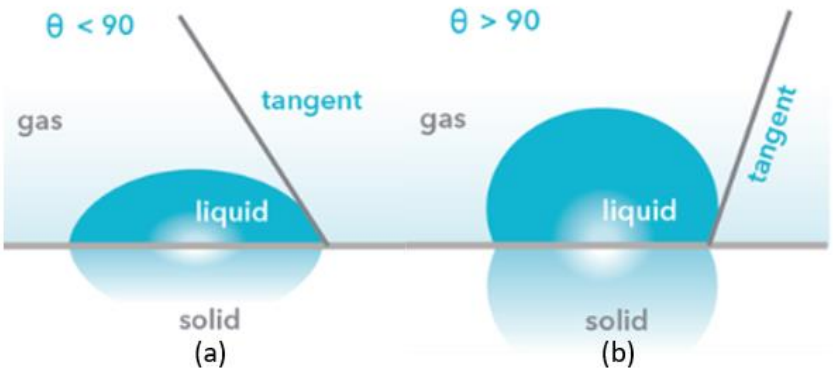

Figure 4: Contact angle of a) wettable surface and b) non-wettable surface [6]

One molecule can have both wettable and non-wettable parts. In this case, the molecule is called an amphiphile [11]. Hexagonal boron nitride is an amphiphile. When the amphiphilic substance is a liquid, it is known as a surface-active agent (surfactant). Ethanol and soap are both surfactants [2]. This means that they will spread out over the surface of an air-water interface instead of falling into the water. It is thermodynamically favorable to have the hydrophilic portion oriented towards the water while the hydrophobic portion is oriented away from the water, towards the air. All three steps, sample injection, Marangoni densification, and transfer occur at the air-water interface instead of in the bulk of the fluid because amphiphiles are the driving constituents of each step in the process.

Surface tension and wettability are important in each subsystem. Surface tension drives the Marangoni effect as soap has a lower surface tension than water. This difference creates a surface tension gradient on the air-water interface after the soap is introduced. The surface energy of various materials and the associated wettability of a surface is key to understanding the material selection process used in choosing a suitable substrate for the transfer subsystem. Lastly, surfactants play a critical role in isolating the dynamics of the process to the air-water interface.

2.2.2 Injection

The injection subsystem must be capable of repeatably delivering a known number of particles from a reservoir to the air-water interface. The simplest way to ensure that a similar number of particles is added to the air-water interface each run is to inject a known volume of a homogenous solution. A major risk that would cause the solution to not be homogenous is sedimentation. Sedimentation is defined as previously suspended particles settling due to gravity [12]. Sedimentation would cause certain parts of the solution to have a higher concentration of particles than others. This would cause a different number of particles to be

injected for a given volume of solution, jeopardizing the consistency of the monolayers. Minimizing sedimentation will allow a consistent number of particles to be injected into the trough for a given volume to ensure that monolayers are consistent trial after trial.

Sedimentation can occur in three locations of the injection subsystem: in the reservoir holding the solution, in the tubing running from the reservoir to the trough, and in the trough itself. Each area has its own sedimentation risk and different ways to mitigate the risk.

Firstly, sedimentation can occur in the reservoir. Here, the two main methods for avoiding sedimentation are using an ultrasonic bath or a magnetic stirrer. An ultrasonic bath, also known as a sonicator, works by blasting the solution with ultrasonic waves. From the waves, thousands of microscopic bubbles are formed that constantly mix the solution as they collapse [13]. Figure 5 shows how the applied pressure from the ultrasonic sound waves create then violently destroy bubbles resulting in a homogenous solution.

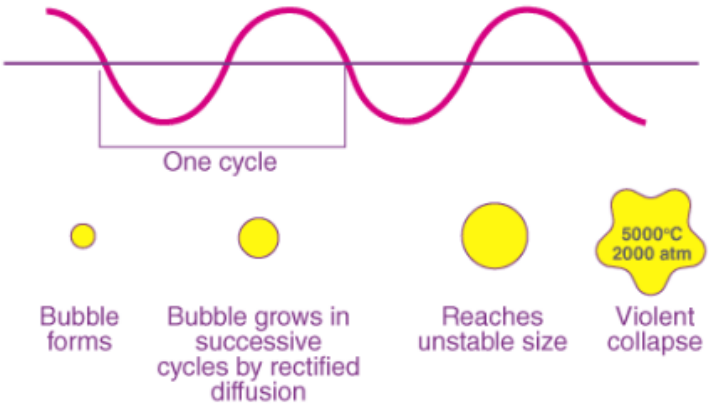

Figure 5: Diagram of sonication [13]

A sonicator is available through Northeastern's DAPS Lab for testing during this Capstone project. However, purchasing one would be cost prohibitive as they can range from $100 to $5000 [14]. For a stand-alone solution, ultrasonic baths are not a cost-friendly solution.

An alternative method of mixing the reservoir is using a magnetic stirrer, which is both cheaper and simpler than a sonicator. A magnetic stirrer is a small magnetic rod that, when put into an electromagnetic field, spins at a set speed to keep a solution mixed [15]. Figure 6, on the next page, depicts the basic components of a magnetic stirrer.

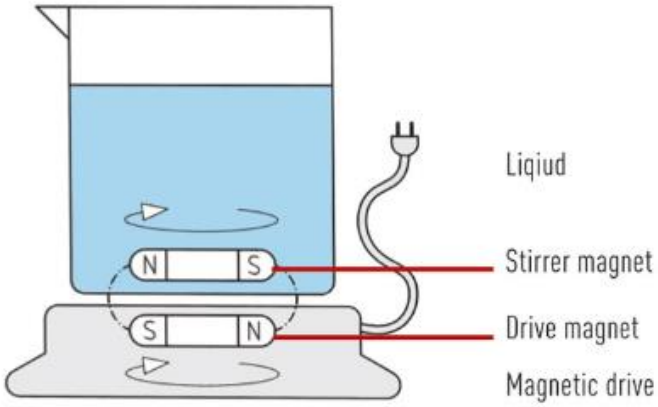

Figure 6: Diagram of a magnetic stirrer [13]

The second area where sedimentation can occur is in the tubing from the reservoir to the trough. In this section, sedimentation occurs when the flow of the fluid is too slow allowing gravity to become the dominating force and push particles to the bottom of the tubing [12]. Therefore, a sufficient flow is required to avoid sedimentation. A formal derivation and substitution of Stokes' law can be used to quantify the issue. Equation 1 can be used to calculate the settling time of the particles in the tubing, or the time it would take for a particle at the top of the tube to settle to the bottom of the tube if flow were to be completely stopped. The equation is defined as:

$$\frac{mg}{6\mu\pi r} = v \qquad (1)$$

where g is gravity, m is the mass of a particle, μ is the viscosity of ethanol, r is the radius of the equivalent volume sphere that the particle would take up, and v is the velocity at which the particle settles [16].

Numerical values were input to the equation to calculate that it will take 11-14 seconds for a 45-micron particle to settle from the top of the tube to the bottom. As this time is shorter than the expected time between trials, it was concluded that the injection tubing must be cleared every run by running the pump in reverse to avoid sedimentation in the tubing.

The final location where sedimentation is a concern is in the trough. When the particles are ejected from the tubing onto the air-water interface, there is a risk of sedimentation if the particles move too far below the surface of the water. The amphiphilic nature of the particles makes them stable once on top of the surface of the water. However, beneath the water's surface, a combination of the upward force due to the ethanol and the downward force of gravity acting on the particles can create a situation where the particles sink to the bottom of the trough instead of rising to the surface [17]. Careful control of the injection angle and speed is required to ensure that the particles do not fall too far beneath the surface of the water. An

injection angle parallel to the air-water interface at a slow speed will cause the particles to have the lowest vertical momentum and therefore the lowest chance of sedimentation.

The major risk of the injection subsystem is sedimentation. Sedimentation in the reservoir, tubing, and trough can be avoided by using a magnetic stirrer, clearing the tubing, and using slow injection speeds, parallel to the interface, respectively.

2.2.3 Marangoni Effect

The Marangoni effect is the movement of particles due to a gradient in the surface tension of two liquids [18]. Marangoni flow is directed from an area of lower surface tension to areas of higher surface tension, as shown in Figure 7.

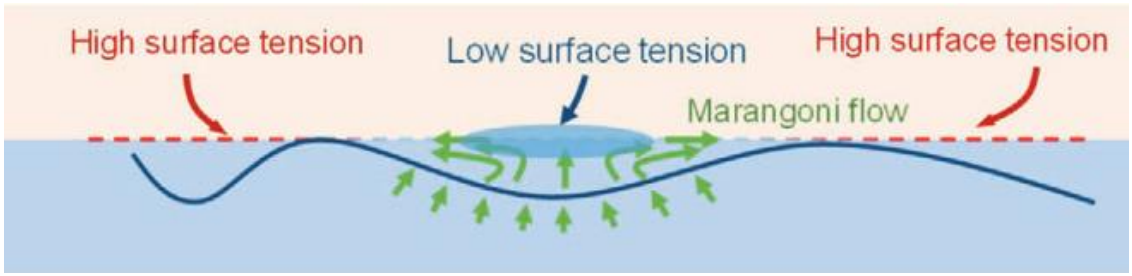

Figure 7: Diagram of Marangoni flow [19]

This flow can be intuitively understood based on the definition of surface tension. Surface tension is related to the cohesive forces that pull like-molecules together. Therefore, the fluid with a higher surface tension has a greater cohesive force than the fluid with the lower surface tension. The result of the mismatch in force is a net movement, or flow, of particles towards the fluid with the higher surface tension.

The Marangoni effect is used in this Capstone project to densify the monolayer. In this case, sodium lauryl sulfate (soap) is used to create the surface tension gradient necessary to cause Marangoni flow, or Marangoni-induced condensation. Soap is both a surfactant and has a lower surface tension than water. For these reasons, when the soap meets the water, it spreads across the surface of the water and drives the particles at the interface away from the region where it was dispensed. Figure 8, on the next page, shows three screenshots of Marangoni-induced condensation of the monolayer at different times after the soap was introduced. A drop of soap is introduced to the left side of the container at time t=0s.

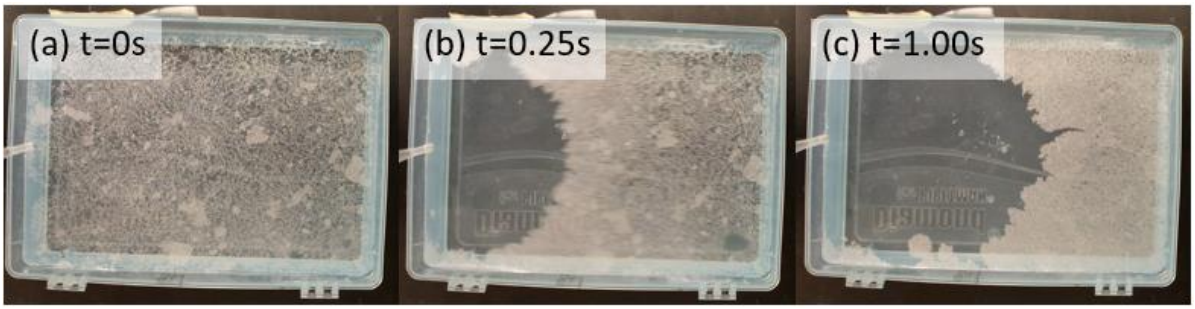

Figure 8: Time progression of Marangoni-induced condensation [20]

After the soap is introduced in panel a), the white hBN particles of the monolayer are driven towards the right side of the container as shown in panel b). The fully densified monolayer is shown in panel c) within a second of adding the soap. Visually, the densified monolayer is opaquer than when the particles were freely floating on the surface. After the Marangoni effect, the water-soap mixture now constitutes the fluid surface, causing the overall surface tension to be decreased at the interface. This allows the monolayer to be more densely packed than is physically realizable upon an interface made up of only water. Therefore, densification via the Marangoni effect theoretically allows for denser monolayers to be manufactured compared to methods that rely on moving particles across interfaces made up of only water.

It is important to note that the Marangoni flow decreases with time as the surface tension concentration is greatest right after the soap is added. As the soap and water mix, the surface tension gradient between the two decreases, resulting in a slower Marangoni flow [19]. This occurs until the soap, a surfactant, has completely spread across the surface of the water and there is no surface tension gradient to induce flow. This means that adding any additional soap will not further densify the monolayer so all soap must be added before any soap is allowed to spread across the entire air-water interface. If a line or a ring of soap was used to induce the Marangoni effect, then tight parallelism tolerances would be required to ensure that soap along the entire shape is added to the interface before the soap diffuses across the surface of the water.

2.2.4 Transfer Methods

The final step of creating a monolayer is to remove the densified monolayer from the air-water interface and transfer it onto a solid substrate where it can be taken for post-processing and inspection. The Northeastern DAPS Lab currently accomplishes this by placing a substrate underneath the surface of the water and dragging the substrate up through the monolayer as was shown in Figure 2, panel c) [2]. This approach has seen success on a small scale, but it is difficult to scale up and automate. Therefore, research was done on how industrial solutions accomplish the transfer of the monolayer onto a substrate.

There are two leading methods for monolayer transfer: Langmuir-Blodgett and Langmuir-Schaefer. The Langmuir-Blodgett transfer method is a vertical dipping technique where the substrate, or sample, is lowered vertically into the monolayer whereas the Langmuir-Schaefer technique is a horizontal dipping method. A diagram of the two techniques is shown in Figure 9.

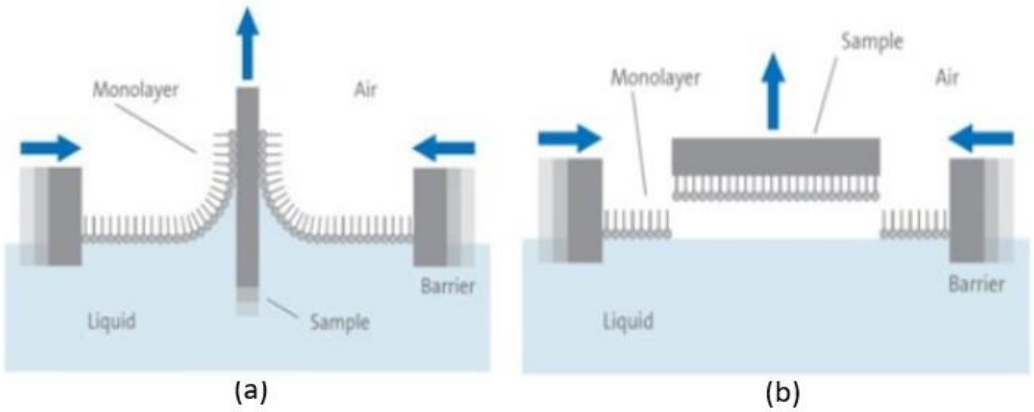

Figure 9: Diagram of a) Langmuir-Blodgett deposition and b) Langmuir-Schaefer transfer [21]

The Langmuir-Blodgett technique relies on moveable mechanical arms that reduce the area of the monolayer throughout the transfer to account for the loss of particles from the water onto to the substrate [22]. The increased complexity of having to control the surface tension during transfer makes Langmuir-Blodgett an unappealing solution.

The Langmuir-Schaefer transfer method was more encouraging for meeting this project's goal of scaling-up and automating the transfer process. The Langmuir-Schaefer technique entails moving a horizontally oriented substrate down until it contacts the monolayer, then pulling the substrate back upwards with the monolayer now stuck to it [23]. There have been no differences in quality reported between the Langmuir-Blodgett and Langmuir-Schaefer transfer methods [11]. Additionally, no mechanical arms or surface tension control are required for the Langmuir-Schaefer method if densification is accomplished using the Marangoni effect.

The main risk associated with the Langmuir-Schaefer technique is properly selecting the material for the substrate. To ensure a good transfer from the water to the substrate, the substrate material must be selected such that the particles will spontaneously transfer from the water to the substrate. The conditions under which the transfer is spontaneous can be determined using Helmholtz free energy [24], which states that the free energy is equal to the internal energy minus temperature times the enthalpy of the system. This equation can be rearranged for the system of water, particles, a substrate, and air to obtain the following requirement for a spontaneous transfer:

$$\boldsymbol{Area} * (\boldsymbol{\gamma_{Air-Water}} + \boldsymbol{\gamma_{Particles-Substrate}} - \boldsymbol{\gamma_{Water-Particles}}) < \mathbf{0} \qquad (2)$$

where γ is the surface energy between the two substances.

There are three terms in this equation, of which only one can be altered by the material of the substrate. To achieve the best possibility of a spontaneous reaction, the surface energy difference between the substrate and the particles must be minimized. Therefore, the free energy of the substrate must equal the free energy of the particles. To ensure that the Langmuir-Schaefer approach has a spontaneous reaction, a substrate with a surface energy like the surface energy of hBN must be determined.

2.3 Products

Langmuir troughs are available on the market as automated ways to create monolayers. It is important to understand what makes these products competitive, as well as what qualities and features they lack to inform the requirements of the design of this Capstone project. The most prominent commercial producer of Langmuir troughs is KSV NIMA, producing a wide variety of sizes and configurations [25]–[27]. The KSV NIMA offers a wide range of sizes for their lab-grade instruments, ranging from a 26mm-by-26mm sample up to a 106-by-106mm sample [25]. An image of the large sized Langmuir trough can be seen in Figure 10.

Figure 10: KSV NIMA Large Langmuir-Blodgett Trough [26]

The Langmuir-Blodgett trough includes surface tension sensors to ensure consistent monolayer density and mechanical guides to condense the monolayer. Langmuir-Schaefer deposition can also be achieved using

this trough by replacing the transfer mechanism with the provided Langmuir-Schaefer mechanism. Additionally, an automatic sample injection apparatus can also be purchased with the trough.

For single-use samples in a controlled lab space, KSV NIMA instruments appear to be epitome of Langmuir troughs; however, this idea quickly dismantles when transferred to industry and production at scale. The maximum sample that KSV NIMA's troughs can coat is only 4.17in-by-4.17in. The requirement for this Capstone project is the ability to coat a 9in-by-9in substrate. Also, KSV NIMA troughs are prohibitively expensive, costing upwards of $30,000 for a base model Langmuir trough and up to $55,000 for high end models [28].

The current market for Langmuir troughs is missing products that offer the Marangoni effect as the densification method. Also, no commercially available products can coat a 9in-by-9in substrate in a single trial. This Capstone market could fill these gaps in the market.

2.4 Background Research Summary

The goal of this Capstone project is to design and build an automated device that replicates the monolayer formation process developed in the Northeastern DAPS Laboratory at a larger scale. This process can be divided into three subsystems, each of which has its own requirements and risks associated with it.

The first subsystem is the injection subsystem, which must mix the particles in an ethanol solution and dispense the particles onto the air-water interface. The major risk of this subsystem is sedimentation which should be mitigated by using a magnetic stirrer in the reservoir, clearing the injection tubing after each run, and minimizing the vertical momentum of particles hitting the interface. The second subsystem is the Marangoni subsystem, which must drop soap into the trough to cause particle densification. The soap must be added all at the same time because once the surface tension of the air-water interface is broken, further addition of soap will not cause the monolayer to densify more. The final subsystem, transfer, must remove the densified particle monolayer off the air-water interface onto a 9in-by-9in solid substrate. The Langmuir-Schaefer transfer technique was identified as the simplest and most applicable transfer method for this Capstone project. The material of the substrate used must be carefully selected so that it causes the monolayer to be spontaneously transferred from the water to the substrate.

Commercially available products offer automated Langmuir-Schaefer transfer methods, but they are not large enough to meet the requirements of this Capstone project. In addition, they do not use the Marangoni effect for densification, inherently limiting the maximum achievable monolayer density. This gap in the current market would potentially make a successful device produced from this Capstone project desirable to companies interested in large-scale monolayer manufacturing.

3 Design

In this section, the entire design will be explored in detail. The design can be split into three subsystems: injection, Marangoni, and transfer. Each subsystem was individually analyzed and optimized such that when all subsystems were combined, they successfully semi-automated the creation, densification, and transfer of the monolayer. The injection subsystem involves adding a solution of hBN and ethanol onto the air-water interface. The Marangoni subsystem induces the densification of the monolayer by introducing soap to the interface. Lastly, the transfer subsystem removes the particles from the interface by depositing them onto a substrate. The following sections will detail the design criteria, iterations, and results from the development of each subsystem. Then, the results of the integrated, scaled-up design will be discussed building upon the individual progress of each subsystem.

3.1 Injection Subsystem

3.1.1 Criteria

The injection subsystem is responsible for delivering a known number of particles from a reservoir to the air-water interface. It is crucial that the injection subsystem can deliver a reliable amount of hBN to the air-water interface to ensure that the quality and size of the monolayers are consistent across runs. Background research illuminated ways to mitigate sedimentation to ensure a homogenous solution of ethanol and hBN. A magnetic stirrer must be included to eliminate sedimentation in the reservoir. A pump capable of running forward and reverse at variable speeds is important to ensure the tubing can both pump the solution into the trough at low speeds and be cleared between runs. Lastly, a tower capable of constraining the angle of the tubing and adjusting the height of the tubing relative to the surface of the trough will diminish concerns of the particles sedimenting to the bottom of the trough upon injection. These criteria alleviate sedimentation concerns establishing that a known volume of solution of hBN and ethanol will correlate to a known number of hBN particles. Therefore, if the pump can reliably output a consistent volume of solution from the reservoir to the trough, the injection subsystem will be able to satisfy its design requirements. Testing the injection subsystem includes visually determining if sedimentation occurs and verifying that the pump can output a consistent volume of solution.

3.1.2 Design 1

The initial design of the injection subsystem centered around using a pump to siphon solution from a reservoir into the trough. The main components of the design were a magnetic stirrer, a reservoir, a pump, tubing, and a tower. A rough sketch of the initial design is shown in Figure 11 on the next page.

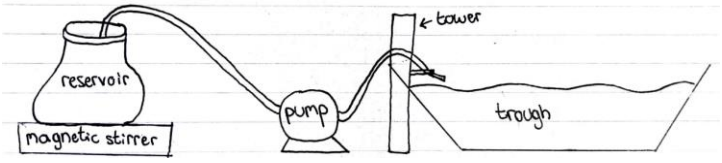

Figure 11: Sketch of injection subsystem

Each component in the design had to be individually determined and sourced. Magnetic stirrers are widely available. One that had variable speed via an onboard potentiometer and came with stirrer bars was purchased [29]. Next, Erlenmeyer flasks were purchased to use as the reservoir. They are made in a wide variety of sizes, which allow easy scaling from the testing stage to the final design as the amount of solution required increases. Additionally, they are specifically designed for the purpose of mixing solutions as they have wide bottoms and relatively short heights [30].

The next component of the design was the pump. A peristaltic pump was determined to be the best pump type for this application. Peristaltic pumps work by periodically squeezing a tube between rollers, moving the desired solution along the length of the tube [31]. The main advantage of a peristaltic pump is that no mechanical components ever contact the fluid. This simplifies maintenance and extends the life of the pump, especially when working with small particles that could erode any mechanical components they encounter. An H-bridge motor controller was purchased to allow the pumps direction and speed to be controlled from a microcontroller. Additionally, silicon tubing with an inner diameter of two millimeters and an outer diameter of four millimeters was selected to interface with the outlet of the selected pump.

The tower was the final component to be designed. The tower needed to be capable of ensuring that the end of the tubing was close to and parallel to the air-water interface in the trough. Also, as the water level in the trough may change, the height of the tower's arm needed to be adjustable. The first design of the injection tower featured an adjustable long arching arm that allowed the tubing to be routed around any size trough.

A diagram of the complete initial prototype is shown in Figure 12.

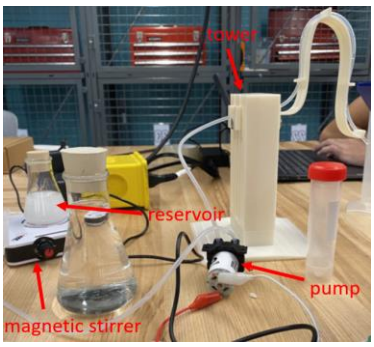

Figure 12: Diagram of initial prototype of injection subsystem.

The first test of the initial design was tested to visually inspect for sedimentation. With the magnetic stirrer, no sedimentation was observed in the reservoir. Sedimentation was observed in the tubing when the pump was not running consistent with the expected results from Stokes law as seen in Equation 1. However, the solution was able to be cleared from the tubing if the pump was run in reverse which left no particles in the tubing to be able to sediment.

The second analysis run on the initial prototype was flow rate testing to determine if the flow rate of the pump was consistent. The tower was adjusted to both its maximum and minimum height to see if the difference in pressure head caused a statistically significant difference in the flow rate. The pump was set to run at its maximum speed for five different durations of time. Each duration of time was tested five times for a total of 25 trials per height. A graduated cylinder was used to measure the volume of solution moved in each trial. A T-test assuming equal variance was run between the data collected at the maximum and minimum heights of the injection tower. The results of this statistical analysis are displayed in Figure 13.

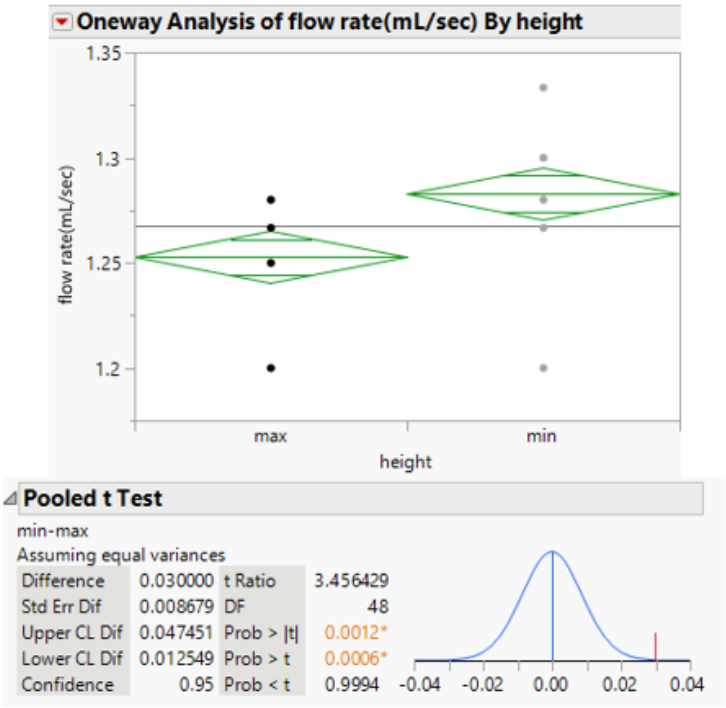

Figure 13: Results of T-test assuming equal variance for flow rate testing at maximum and minimum heights

The test statistic was 0.0012, much lower than the 0.05 cut off value. This means that there is a statistically significant difference between pump performance at the maximum and minimum test heights. Therefore, the flow rate of the pump is dependent on the height of the adjustable tower and more testing would have to be done to characterize the relationship between tower height and flow rate.

Another result from this flow rate validation test was that large amplitude vibrations were observed in the arm of the injection tower. The length and thickness of the arm made its natural frequency close to the driving frequency of the pump, which led to violent vibrations. Vibrations are not desirable as they lead to excessive wear and short lifetimes of components.

Takeaways from this initial design of the injection subsystem were that the pump and magnetic stirrer worked as required. The pump was able to consistently move the solution through the tubing as well as clear the tubing by running the pump in reverse. The magnetic stirrer successfully homogenized the solution in the reservoir. However, the injection tower did not function as desired. The tower's excessive height and length lead to inconsistent flow rates at different heights and excessive vibration in the arm. Therefore, only the injection tower had to be improved for the next iteration of the design.

3.1.3 Design 2

The second design of the injection subsystem featured a newly designed injection tower that not only reduced bulk of the first tower's design, but also reduced vibrations. The overall volume and material used was greatly reduced as the first design had an excessive amount of adjustability and bulk. The newer injection tower enabled three inches of adjustability in the height of the arm compared to the six inches of adjustability featured in the previous iteration. Next, the length of the adjustable arm was significantly reduced to make the design more resistant to vibrations induced by the pump. The final improvement in the tower was that the exit angle of the pipe from the adjustable arm was made much closer to parallel. This significantly reduced the vertical momentum of the particles to reduce the risk of sedimentation of the particles to the bottom of the trough. Figure 14 shows an image of the redesigned injection tower.

Figure 14: Design 2 of the injection tower

The flow rate testing done on the first design was repeated to ensure that the second design eliminated the inconsistency in flow rates based on the arm height. The statistical results are shown in Figure 15.

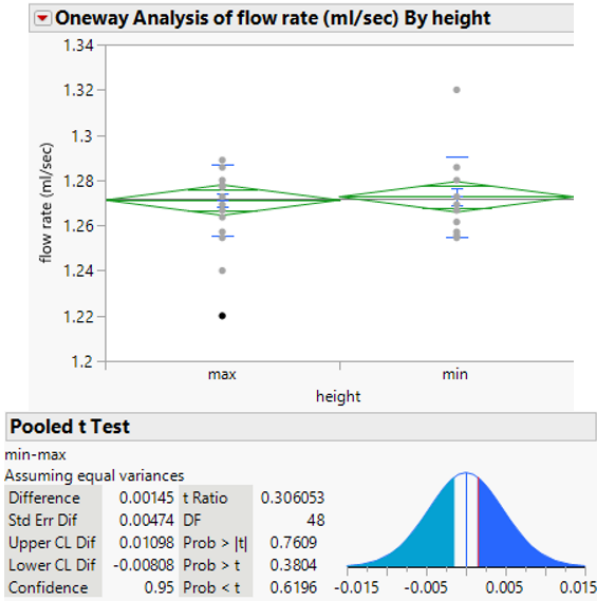

Figure 15: Results of T-test assuming equal variance of design 2 of the injection subsystem

The test statistic between the flow rate at the maximum and minimum heights of the tower was 0.7609. This value is greater than the confidence level of 0.05, supporting the null hypothesis that said the height of the arm did not have a statistically significant effect on the flow rate. Therefore, a single flow rate value can be used regardless of what height the arm is set to.

The second issue with design 1 was the excessive vibrations of the arm. Vibration analysis was run on both the first and second designs of the injection tower to compare their vibrations and alleviate vibration concerns in design 2. The results of the vibration analysis for both design 1 and 2 is shown in Figure 16.

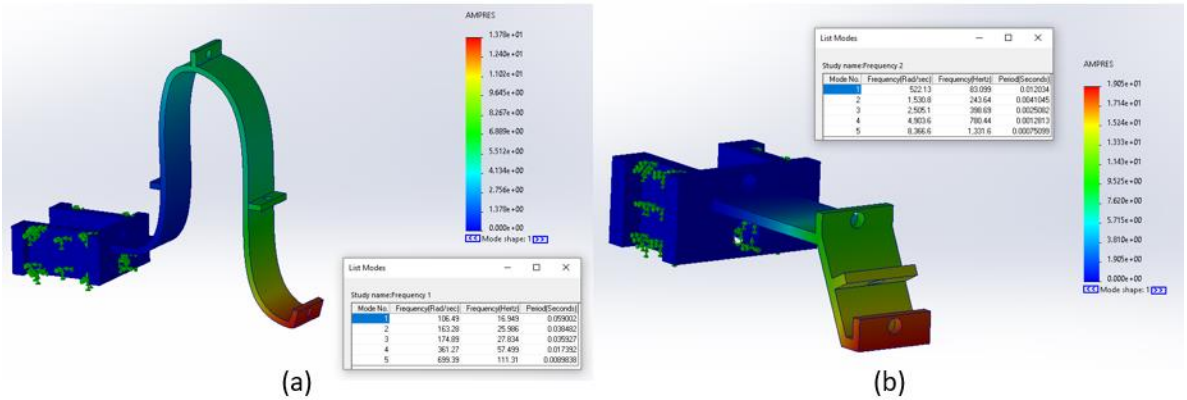

Figure 16: Vibration analysis of (a) design 1 and (b) design 2

The natural frequency that caused the first mode of vibration for designs 1 and 2 were 16.949 Hz and 83.099 Hz, respectively. Design 2 raised the natural frequency by almost a factor of 5. The natural frequency of design 1 is similar to the driving frequency of the pump, which is why design 1 showed excessive vibrations. However, design 2 has a much higher natural frequency than the driving frequency of the pump, so the first mode of vibration is not excited. This analysis agrees with physical results of that the second design did not suffer from high vibrations during the second flow rate test.

Design 2 of the injection tower alleviated concerns regarding flow rate inconsistency and unwanted vibrations. With a suitable tower, the injection subsystem could be integrated with the large-scale design.

3.2 Marangoni Subsystem

3.2.1 Criteria

The Marangoni subsystem must add soap onto the air-water interface to induce the densification of the monolayer. A successful Marangoni subsystem will reliably and repeatably densify the particles so that a high-quality monolayer is formed in the same location of the trough, every time. The resulting densified monolayer must also be homogenous. This means that all parts of the monolayer must be uniformly dense without any cracks or low-density regions.

3.2.2 Marangoni Shape Considerations

In the initial demonstration done in the DAPS lab, a single drop of soap was used to induce the Marangoni effect. However, this method caused cracks to be formed in the densified monolayer as can be seen along the edges of the monolayer in Figure 2, panel c. To reduce the risk of the cracking, the Marangoni subsystem must be shaped so that particles densify inwards instead of outwards like the drop of soap does.

Two designs were proposed for the shape that induces the Marangoni effect: a circular ring and a straight line. These two shapes would be coated in soap and lowered into contact with the monolayer. The circular ring, with a diameter of at least 12.727 in, would be used in conjunction with a circular trough to cause densification of the monolayer radially inward from the walls of the trough. A straight-line design, with a length of 9 in, would be used with a square or rectangular trough to cause densification from one end of the trough towards the other. Both densification methods would cause all the particles to be either moving parallel with or towards each other, not away from each other. Therefore, no cracks should be created because of particles pulling away from each other.

A major differentiator between using a circle or a line to induce the Marangoni effect relates to the minimum possible waste that can be accumulated. Waste is defined as particles left on the air-water interface after

transfer. The substrate is going to be a 9in-by-9in square. Therefore, if a circle is used then the substrate must be circumscribed within the circle. The minimum percentage of waste over the area for a line and circle was calculated, assuming a 25 mm tolerance between the edges of the densified monolayer and the substrate. Figure 17 highlights the area of waste for the circle and line design.

Figure 17: Waste (in red) of different Marangoni shapes: (a) circle and (b) line

The minimum percentage waste for the circle and line designs were 52.22% and 32.67%, respectively. This means that the line design has nearly 20% less waste compared to the circle design. Therefore, the line design was decided upon to use for testing. In small-scale testing, a straight-line design was able to uniformly densify the monolayer without showing any signs of cracking.

3.2.3 Marangoni Parallelism Considerations

To ensure that a given Marangoni shape induces uniform densification of the monolayer, all the soap from the shape must be added to the air-water interface before any soap is able to diffuse across and saturate the entire interface. This means that both ends of the line must contact the water in less time than it takes for the soap to travel the length of the line, 9 in.

To understand how this requirement impacts the design of the Marangoni subsystem, the speed of soap had to first be determined. A rudimentary experiment was conducted to determine the approximate speed of soap traveling across the air-water interface. Images were obtained from a slow-motion analysis of the densification process after a line of soap was added to one end of the trough. Figure 18 on the next page shows the screenshots of the densification process.

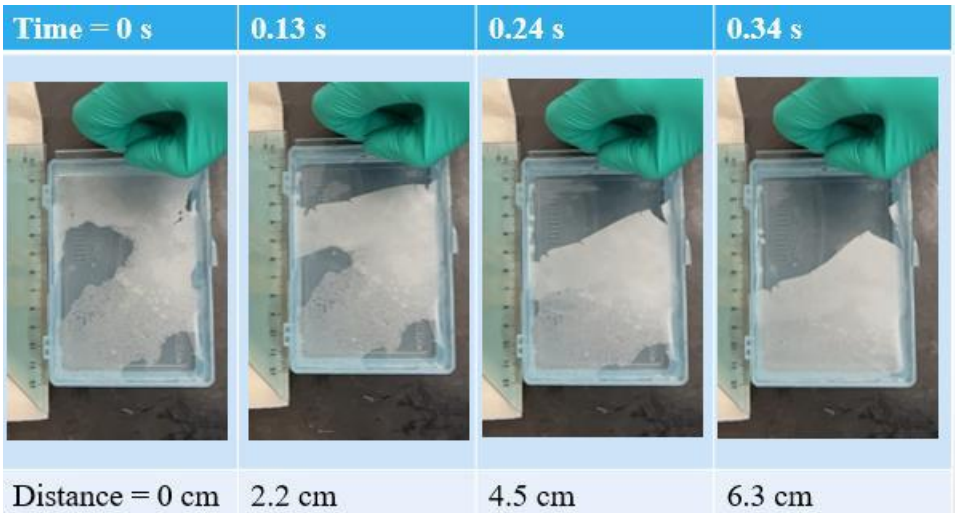

Figure 18: Screenshots of monolayer densification

A plot of the distance the monolayer moved as a function of time was created as shown in Figure 19.

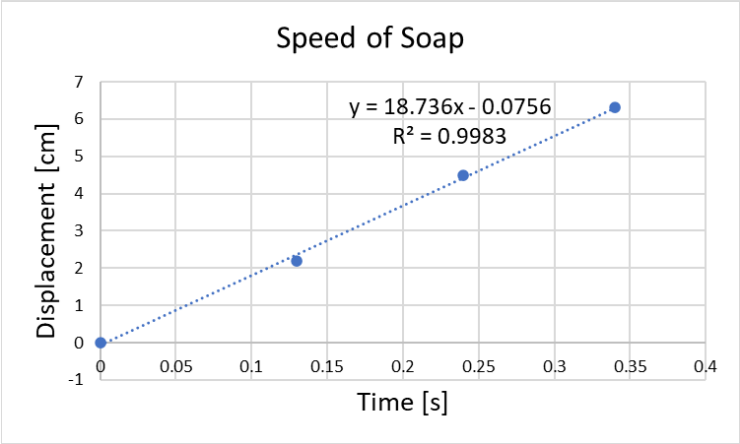

Figure 19: Linear regression of displacement over time

The slope of the linear regression is the approximate speed of soap traveling across the interface. Therefore, the calculated speed of soap is on the order of 18.7 cm/s. The means that the soap will traverse a 9 in length in approximately 1.22 seconds. If the line of soap moves at a vertical speed of 500 mm/min or 0.328 in/sec, then the maximum allowable difference in height between the two ends of the substrate is 0.40 in. This corresponds to a maximum allowable angle between the line and the surface of the water of 2.548º. A parallelism tolerance of 2.548º is easily achievable with bubble levels and two-point adjustment. Therefore, parallelism tolerance of the Marangoni line is not a concern with the large-scale design.

3.3 Transfer Subsystem

3.3.1 Criteria

The transfer subsystem is responsible for removing the monolayer off the air-water interface and depositing it onto a solid substrate. The Langmuir-Schaefer transfer method was identified through research and decided upon as the transfer method that would be fine-tuned in this Capstone project. The Langmuir-Schaefer method created many constraints for the transfer subsystem. First, the substrate must be horizontally suspended without any mechanical parts beneath it. This must be done so that no mechanical parts disrupt the monolayer before the substrate contacts it. Additionally, the design must be capable of moving at speeds less than 1 mm/min with positioning repeatability no greater than 0.1 mm. Next, the parallelism of the substrate must be tightly controlled to ensure that the substrate contacts the monolayer in a predictable fashion. This means that the pitch, roll, and z-axis of the substrate must be adjustable. Other criterion included that the design should be capable of using a standardized of-the-shelf substrate and there should be an easy way to mount and dismount the substrate. If all these criteria are met, then the transfer subsystem should be capable of achieving its goal of reliably picking up the densified monolayer from the interface without disturbing it.

3.3.2 Transfer Design Brainstorming

The team began brainstorming designs for the transfer subsystem by reviewing mechanisms that enabled control over the vertical motion, pitch, and roll of a substrate. An early observation was that the proposed Langmuir-Schaefer technique has similar functional requirements as SLA 3D printers. A machine such as the Formlabs Form 3, shown in Figure 20 on the next page, features an inverted z-axis build plate that allows parts to be created on the bottom of the platform [32]. An SLA 3D printer accomplishes the design criteria that there cannot be any mechanical components beneath the substrate in a simple and well-proven way. There is a single linear actuator that drives the motion of the build plate, which simplifies the controls and electronics required compared to a device that has multiple actuators. In addition, SLA 3D printers require high levels of positioning repeatability proving that this design also satisfies the design requirement of having a positioning repeatability of at least 0.1 mm.

Figure 20: Formlabs Form 3 SLA 3D printer [32]

A design like an SLA 3D printer would be centered around a single linear actuator that moves the substrate up and down. The next design decision is how to control the pitch and roll of the substrate. The two competing ideas were to ensure parallelism of the substrate and the water through a tolerance stack up and ensuring parallelism by an adjustable leveling system. Based on advice from an external design reviewer, Andrew Caunter, it was determined that an adjustable mechanism would be the easiest way to reach the parallelism tolerances [33]. A tolerance stack up approach would be too difficult to achieve given the budget of Capstone. The mechanical mechanism that allows adjustment of the pitch and roll of the substrate is called a kinematic mount as shown in Figure 21. The three set screws can be independently loosened or tightened to create a range of pitch and roll angles.

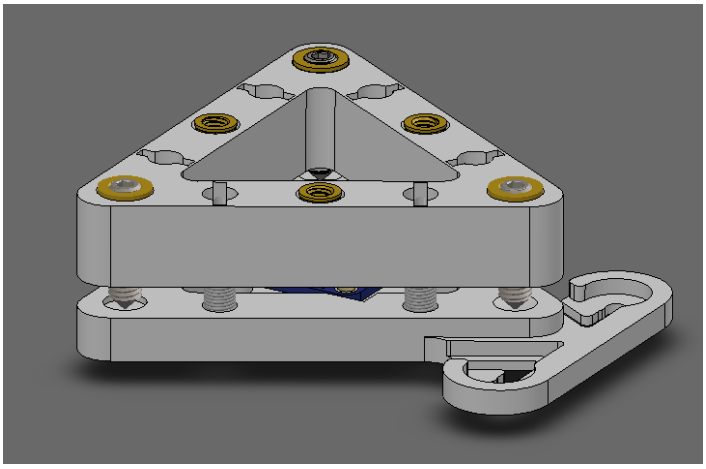

Figure 21: Kinematic mount

The combination of the linear actuator for the z-axis positioning and the kinematic mount for the pitch and roll satisfied all degree-of-motion requirements for the transfer subsystem while minimizing complexity. There is only one electrical component, the linear actuator, and only a few mechanical components required to interface the kinematic mount with the linear actuator.

The final two design criteria that had to be brainstormed were how to use off-the-shelf substrates with limited modifications and make them easy to attach and detach from the machine. Using off-the-shelf substrates means that they can be bought in bulk without having to do any machining to the substrates before they are used. The most popular commercially available Langmuir-Schaefer trough, produced by KSV NIMA, uses vacuum suction cups to grip the substrate [25]. Vacuum suction cups allow for any substrate to be easily added and removed, but they require a complicated pneumatic system. Additionally, the positioning repeatability of the mounting process with suction cups would be highly variable depending on how hard the operator compressed the suction cups. An opposing idea for mounting and dismounting the substrate was to use magnets. Magnetic tape would be added to the topside of each substrate and the bottom of the machine so that substrate could be easily added and removed with minimal amount of variation. Magnetic tape would require a small amount of substrate modification but would remove the need for a pneumatic system and would improve positioning repeatability. Therefore, magnetic tape was chosen as the mounting method.

The basic aspects of the initial brainstormed design were a linear actuator to control the height of the substrate, a kinematic mount to adjust the pitch and roll of the substrate, and magnets to allow the substrate to be easily attached and detached. The next step in the design process was to tune the parameters of the Langmuir-Schaefer method to make it reliable and repeatable.

3.3.3 Substrate Selection Testing

The first parameter of the Langmuir Schaefer technique was what material should be used as the substrate. This material had to be selected such that it would create a spontaneous transfer of the monolayer from the air-water interface to the substrate. Recall from analysis of Equation 2 of the Helmholtz free energy of the system that the desired material is one that has a free energy as similar to the free energy of hBN as possible. Based on literature, hBN has a contact angle of 83° [34]. This means a slightly hydrophilic material should have the highest transfer success.

Four materials with varying surface energies were selected to test: polytetrafluoroethylene (PTFE), polypropylene (PP), polyvinyl chloride (PVC), and polyethylene (PE). Polymers were chosen due to their availability at scale which would allow sourcing a 9in-by-9in substrate to be easy. The contact angles of

each of the four potential substrate materials were measured using a goniometer. A goniometer works by carefully aligning the camera with the substrate to take a clear image when a drop of water is placed on the substrate. Additionally, a polarizing box, not pictured, is placed between the light source and the camera to obtain sharp contrast between the water droplet and the air. An image of the goniometer used is shown in Figure 22.

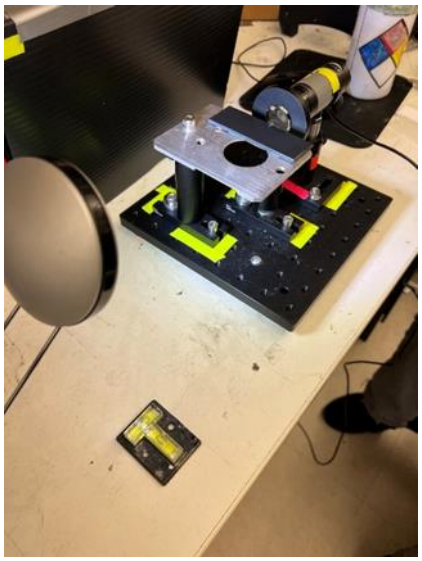

Figure 22: Image of goniometry setup

Images of the droplet of water on each substrate are shown in Figure 23 and the numerical results are summarized in Table 1.

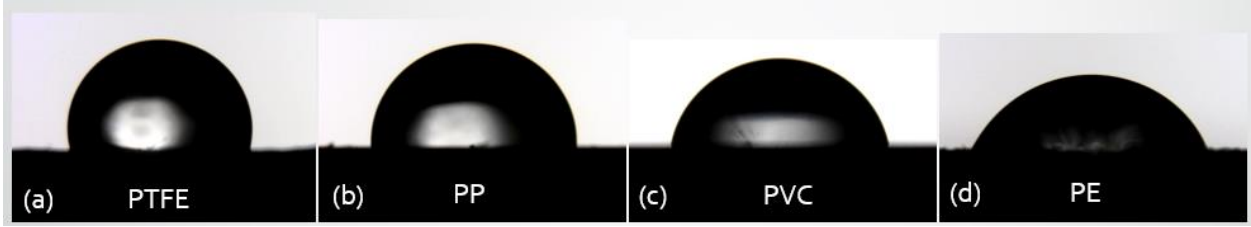

Figure 23: Goniometry images of various materials: (a) PTFE, (b) PP, (c) PVC, and (d) PE

Table 1: Contact Angles for Various Substrates

Substrate Material	Contact Angle (º)
PTFE	95
PP	90
PVC	77
PE	68

Based on the goniometry measurements, PVC has the contact angle most like hBN with a difference of six degrees more hydrophilic. PE has the least similar contact angle to hBN with a difference of 15 degrees more hydrophilic.

With the surface energies of each substrate determined, they could be tested to see which substrate had the greatest success in transferring the monolayer off the air-water interface. The transfer ratio is used to quantify the success of the transfer. The transfer ratio is defined as the area of the substrate covered by particles after the transfer divided by the total area of the substrate [35]. A high transfer ratio is desired with unity being the optimal transfer ratio.

The experimental procedure for testing the different substrates involved obtaining two 3in-by-1in samples of each material. The samples were sonicated in iso-propyl alcohol for five minutes to clean them. Then, one-by-one, the samples were mounted onto the prototype using magnetic tape and lowered into a trough with a densified monolayer. The trough was sanitized using isopropyl alcohol in between every trial run. The speed of the substrate going down into the trough and rising from the trough was 1.2 mm/min for both directions. An image of the experimental setup and small-scale prototype featuring the linear actuator and kinematic mount is shown in Figure 24. In the image, a team member is adding hBN into the trough prior to testing a sample.

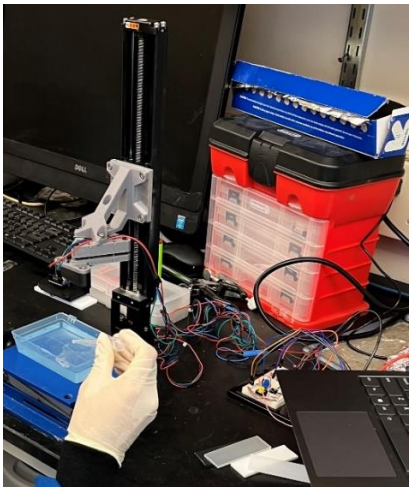

Figure 24: Experimental setup for substrate selection

The results of both trials for each material are shown in Figure 25 on the next page.

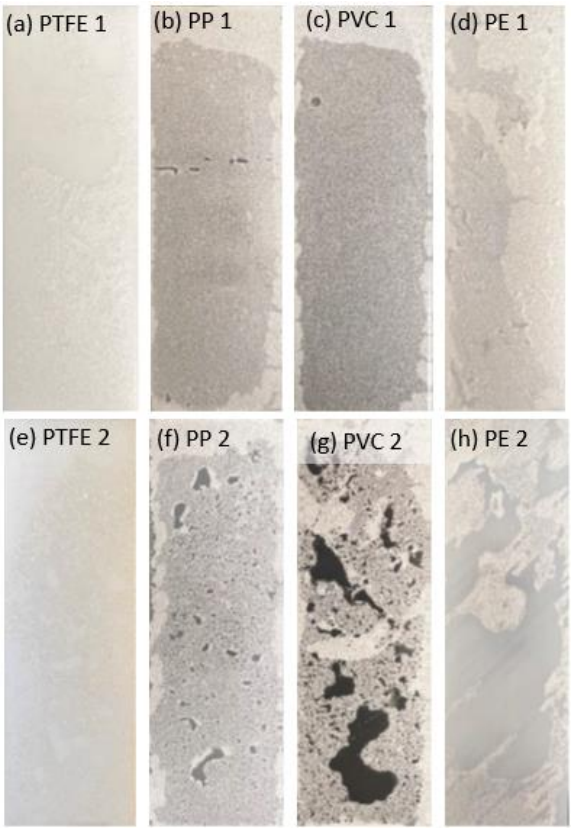

Figure 25: Images of various materials post transfer: (a)-(d) sample 1 and (e)-(h) sample 2

Based on the images, it is qualitatively clear that PP and PVC had more uniform and complete coatings compared to PTFE and PE. This result agrees with Helmholtz energy argument as PVC and PP have contacts angles closer to hBN compared to PTFE and PE. The first samples of PP, shown in panel (b), and PVC, shown in panel (c), had exceptionally uniform coatings with few holes.

An unexpected result from this experiment was that the second samples of all the materials except for PTFE had lower transfer ratios than the first sample. The experimentation order was that the first sample of all the substrates was tested then the second sample of all the substrates were tested. This suggests that a confounding variable was changed between when the first samples were tested and when the second samples were tested.

Analysis of slow-motion video of the transfer offers a possible confounding variable between the first and second rounds of experimentation. As the substrate is raised out of the water with the monolayer on it, the water is still attracted to the monolayer. Therefore, the substrate much reach a certain height above the water's surface before the water detaches from the monolayer. This detachment is very unpredictable and occurs at different locations on the substrate until eventually no water is attached to the monolayer. In the first round of samples, the water seemed to drain off to one side then break off at a corner. This process

was slow and produced few waves in the water. However, for the second round of samples, the water seemed to suddenly break off in random locations around the monolayer, leading to large waves in the trough. These sudden breaks in the water can be roughly correlated to locations where holes developed on the substrate, especially for the second sample of PVC and PE. It is theorized that during the initial set of samples, the parallelism was slightly off leading to one corner being lower than the others. This created an energy minimum where the water could drain to. However, the parallelism for the second set of samples was inadvertently changed leading to no clear energy minimum of the substrate being formed causing the water to unpredictably break off at random points.

The difference in the tilt of the samples can be attributed to the accuracy of the accelerometer. The accelerometer only gave angle measurements to roughly +/- 1°. This means that the parallelism of the substrates could have changed by as much as 1° without the accelerometer accurately measuring the change. Therefore, a more accurate mechanism for determining the angular alignment of the substrate is necessary.

The main takeaways from the first small-scale prototype and substrate selection testing were that magnetic tape was a secure and easy way to mount and dismount the substrates, PVC and PP were the most successful materials in transferring the monolayer, and that the tilt of a substrate must be further investigated with an instrument more accurate than an accelerometer.

3.3.4 Tilt Testing

Small angular misalignment between the substrate and the water is suspected to have improved transfer success in the first test. However, it is theorized that near perfect angular alignment caused holes to form on the substrate since no clear energy minimum was present on the substrate. The goal of this experiment was to determine if repeatable water drainage as the substrate is lifted out of the water can be achieved by slightly altering the pitch and roll of the substrate relative to the water. The pitch and roll of the substrate were altered by the same tilt angle causing one corner on the substrate to be lower than all the rest, creating an energy minimum at that corner. The hypothesis was that the water will be attracted towards the energy minimum and therefore drain in a reliable and repeatable manner without creating any holes in the monolayer. A diagram of the tilt angle experiment is shown in Figure 26 on the next page.

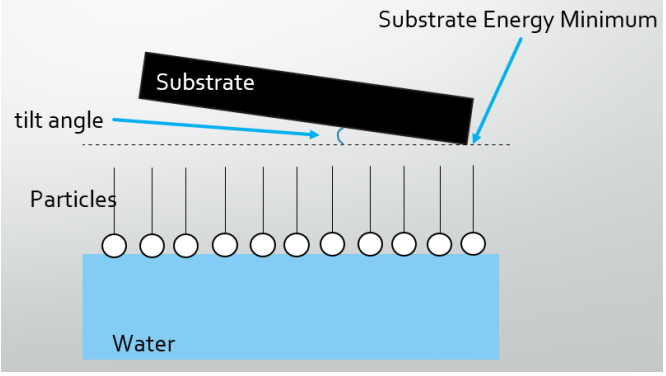

Figure 26: Diagram of tilt test

The experiment was carried out with a slightly redesigned small-scale prototype that used a bubble level to measure the pitch and roll rather than an accelerometer. A CAD rendering of the redesigned prototype is shown in Figure 27.

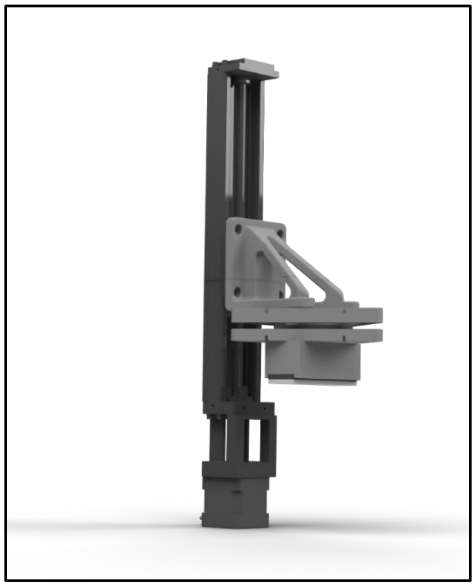

Figure 27: CAD of second iteration of the small-scale prototype

Three different tilt angles were studied, each one for a sample of PP and a sample of PVC. The three tilt angles were 0°, 0.9°, and 1.8°. Like in the first experiment, the substrates were sonicated in isopropyl alcohol prior to transfer to clean them and the trough was sanitized in between trials to limit contamination. The down speed of the transfer was set at 2 mm/min and the up speed was set at 1 mm/min. The results of each transfer are shown in Figure 28 on the next page.

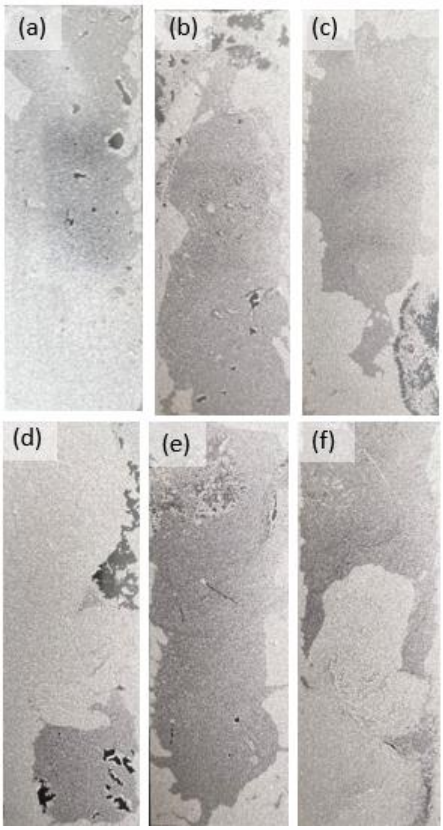

Figure 28: Images of tilt test results: (a) PP 0°, (b) PP 0.90°, (c) PP 1.80°, (d) PVC 0°, (e) PVC 0.90°, and (f) PVC 1.80°

Some things to note on these results are that the PP tilt sample has holes at the top because the monolayer on the air-water interface was not large enough to fully coat the substrate. Those holes are not reflective of the transfer. Also, the disturbance on the PP slanted sample is a fingerprint which was caused by mishandling the sample after the transfer and is also not reflective of the transfer success.

The first conclusion that can be drawn from this experiment is that all six transfers look relatively successful, providing confirmation that the Langmuir-Schaefer technique can be reliable. The second conclusion is that the 0.90° tilt angle resulted in the highest quality monolayer. There are more holes in the PVC 0° sample compared to either the PVC 0.90° sample or the PVC 1.80° sample, indicative of the fact that the water did not have a clear energy minimum to drain to. The 1.80° samples showed ridges forming due to the high shear between the monolayer and water at the higher tilt angles. The 0.90° samples showed neither the increased number of holes that the 0° samples showed, nor the ridges seen in the 1.80° samples. Analysis of the slow-motion videos showed that indeed the 0.90° tilt angle caused a slow and repeatable drainage of the meniscus to the energy minimum of the substrate.

An additional observation about the images in Figure 28 is that the transferred monolayer appears to be dichromatic, or two-toned. There is a lighter, whiter section and then a darker section on most of the substrates. To understand why this dichromatic effect occurs, it is necessary to view the microstructure of the samples. Shows microscopic images of the PVC 0° sample.

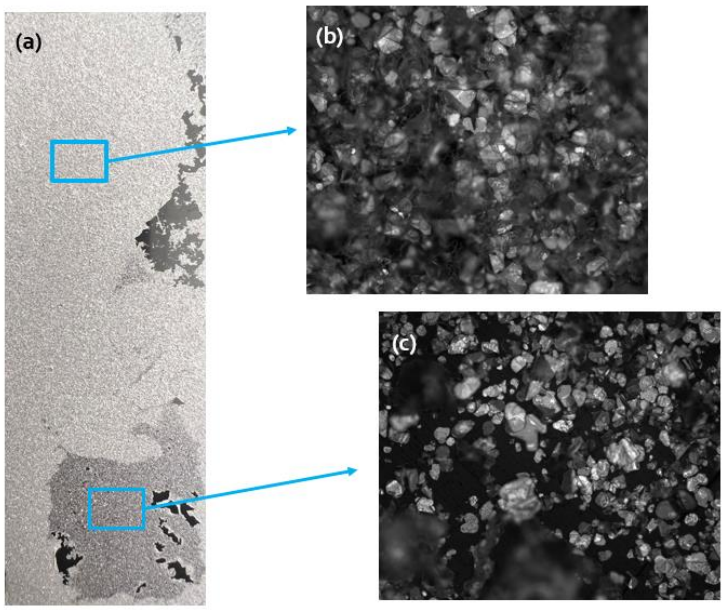

Figure 29: Microstructure of plat PVC sample with (a) macroscopic image of the sample, (b) 20x microscopic image of the lighter section, and (c) 20x microscopic image of the darker section

The microscopic image of the lighter section shown in panel (b) has more fuzzy parts compared to the image of the darker section shown in panel (c). Under a microscope, it is obvious that the lighter section is not a monolayer but a bilayer or potentially even more layers. The focused sections of the darker section are true monolayers, a single layer of particles. It is suspected that the bilayer is formed during the Marangoni step where excessive densification causes particles to overlap. For the application of hBN monolayers as heat sinks that do not interfere with radio frequencies, a monolayer is desired as it is thinner than a bilayer, meaning that it has less interference with radio frequencies. However, the difference between radio frequency transmission between a monolayer and bilayer is not significant enough to be a cause of concern for this project. A substrate fully coated in a combination of monolayer and bilayer sections will still be considered a success [20].

The conclusions of this experiment show that the substrates tilted at an angle of 0.90° had consistent and reliable water drainage. For a large-scale prototype, a 0.90° tilt offset from parallel with the water should be used.

3.4 Final Design

The final design was built upon the successes of testing of each of the individual subsystem. The injection, Marangoni, and transfer subsystems were integrated with an aluminum 8020 frame and electronics. Figure 30 shows a CAD rendering of the final design and Figure 31 shows an annotated exploded view of the design.

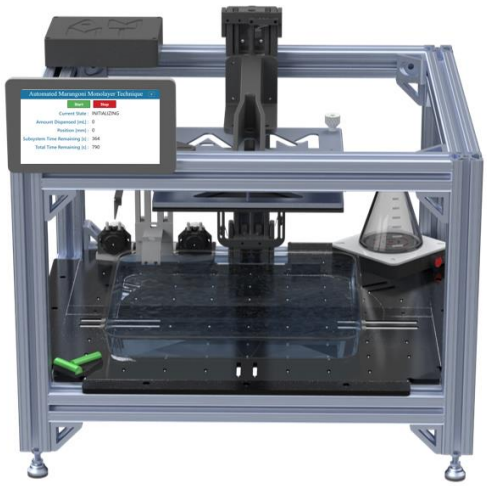

Figure 30: CAD render of the final design

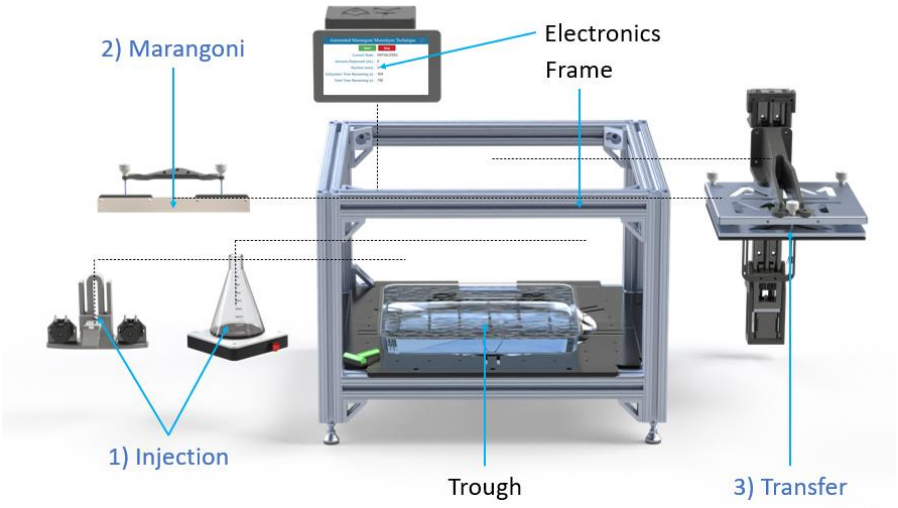

Figure 31: Exploded view of the CAD of the final design

The driving idea behind the full-scale design was adjustability. Many parameters were determined only from experimental testing of the final design such as parallelism, heights, and flow rates. It is important to design with adjustability in mind so that these parameters can be finely tuned without having to manufacture entirely new parts. One place where adjustability in the design is evident is in the many mounting holes,

both on the gantry plate of the transfer subsystem and on the base plate. This allows additional tools and instrumentation to be added in to aid in testing as needed. Another adjustable feature is the use of aluminum T-slot extrusion as the frame, which permits the fast and secure mounting of auxiliary hardware and electronics using T-slot nuts.

The concept of adjustability was also included in the redesign of each subsystem when it was altered to easily integrate with the final design. All subsystems have some built-in leveling and adjustment. The injection subsystem has an adjustable height arm to tune how close the tubes are to the interface. The Marangoni subsystem has slots to mount it to the gantry plate, allowing adjustment of how far the Marangoni line sticks out from the substrate. Lastly, both the Marangoni and transfer subsystems have thumbscrews that allow their levels to be finely adjusted. An annotated render of each scaled-up subsystem is shown in Figure 32.

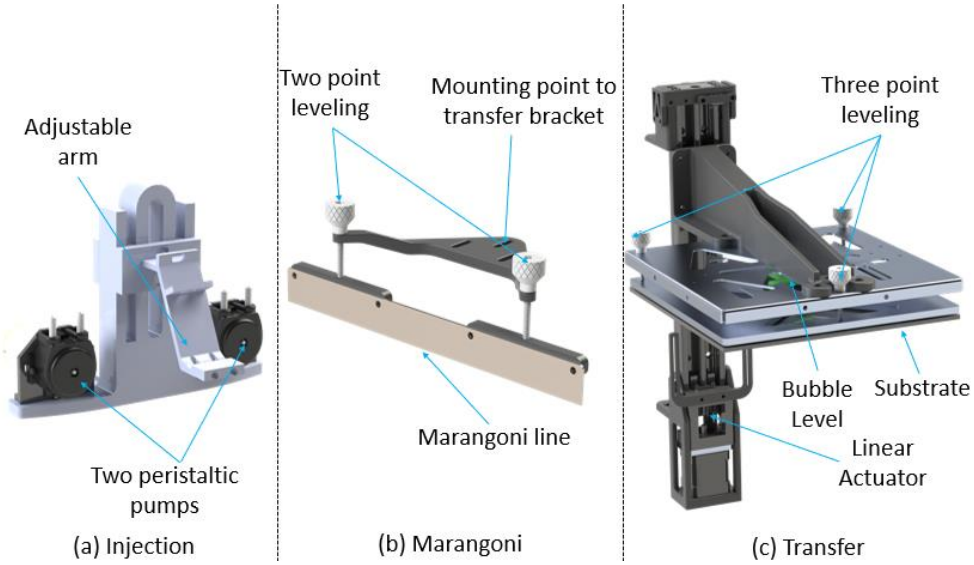

Figure 32: Annotated CAD of a) injection, b) Marangoni, and c) transfer subsystems

In addition to the redesigned subsystems, electronics had to be designed to integrate the operation of all subsystems so that the manufacturing process could be automated. An ESP32 microcontroller was selected to work with the motors that control the injection pumps and the linear actuator. In addition, a Raspberry Pi with a touchscreen was used to host a Python-based user interface. The user interface allowed for easy configuration and operation of the device. A schematic of the electronics is shown in Figure 33 on the next page.

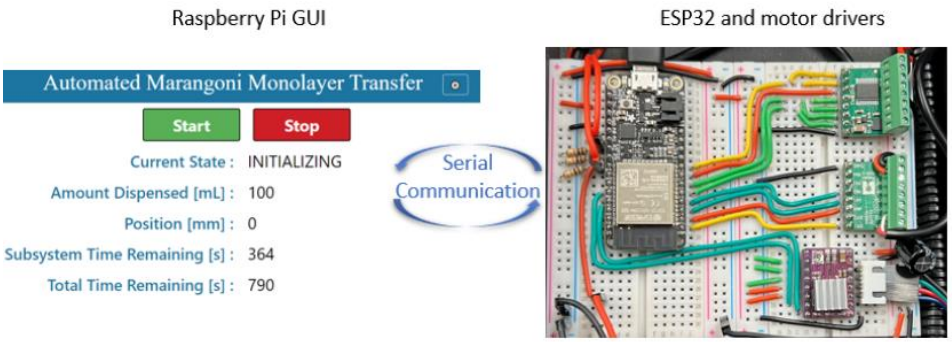

Figure 33: Schematic of electronics

3.5 Execution of Final Design

The final design was constructed from a combination of off-the-shelf, custom waterjet, and 3D printed parts. All components were easily put together with minimal redesign. An image of the physically constructed final design is shown in Figure 34.

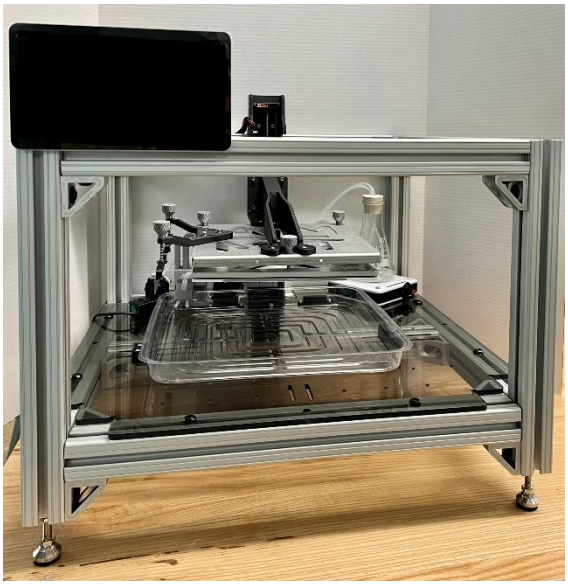

Figure 34: Image of the final design

The first step to making the fully constructed large-scale prototype operational was calibration. First, all adjustable features had to be tuned such as ensuring the substrate had a tilt angle of 0.90°, consistent with the results of small-scale testing. Additionally, variables in the code had to be updated to match the physical system such as the heights between the Marangoni line and the substrate as well as the injection time and transfer speed. Since the final design was created to be adjustable, tuning all these mechanical and software-based parameters was straightforward.

After the system was precisely tuned, tests were performed. The testing procedure had a few manual set-up and clean-up tasks but was largely automated. To begin, a new, clean trough was filled with 1600 mL of water, the Marangoni line was coated with soap, and a clean substrate was mounted. After those manual steps, the start button was pressed on the touchscreen. This began the automated creation process of the monolayer. First, the particles were injected onto the interface. Then, the Marangoni line was lowered into contact with the interface to induce the densification of the monolayer. Lastly, the substrate was lowered into contact with the monolayer and then slowly lifted with the particles now stuck to it. Images of the automated process are shown in Figure 35 . Finally, the manual clean-up steps were to remove the substrate from the mount and to drain the trough.

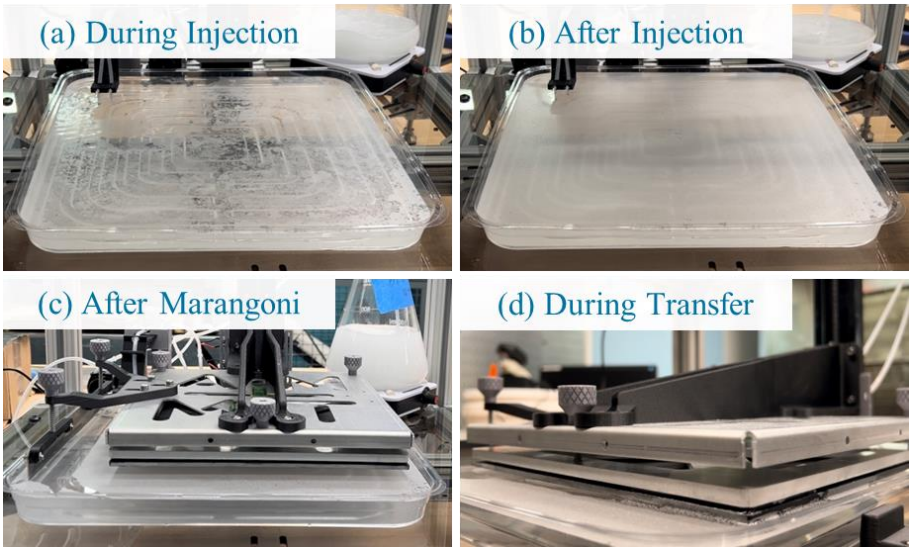

Figure 35: Images of the automated monolayer creation process

A few unforeseen challenges arose during testing. First, contamination of the trough was a major problem. Recall that the Marangoni effect works based on a gradient in the surface tension of the interface. If the surface tension of the air-water interface was already reduced due to contamination, then no Marangoni-induced densification would occur. For this reason, great care was taken to make sure that a clean trough was used every time and no extraneous objects contacted the air-water interface before the Marangoni-line did. Another issue arose from vibration. The environment where these tests were conducted was near a machine shop which caused visible vibrations on the water's surface. It is suspected that these vibrations reduced the homogeneity of some monolayers as the water's surface had ripples and was not flat. To reduce vibratory concerns, the magnetic stirrer was shut off when transfer began, and testing was completed when the machine shop was closed.

Each time the team experienced a failed test, one parameter of the process was changed for the next trial. This iterative tuning of the system continued until a fully coated 9in-by-9in monolayer was created. Figure 36 below shows images of some of the failed initial tests along with what the suspected issue with the test was.

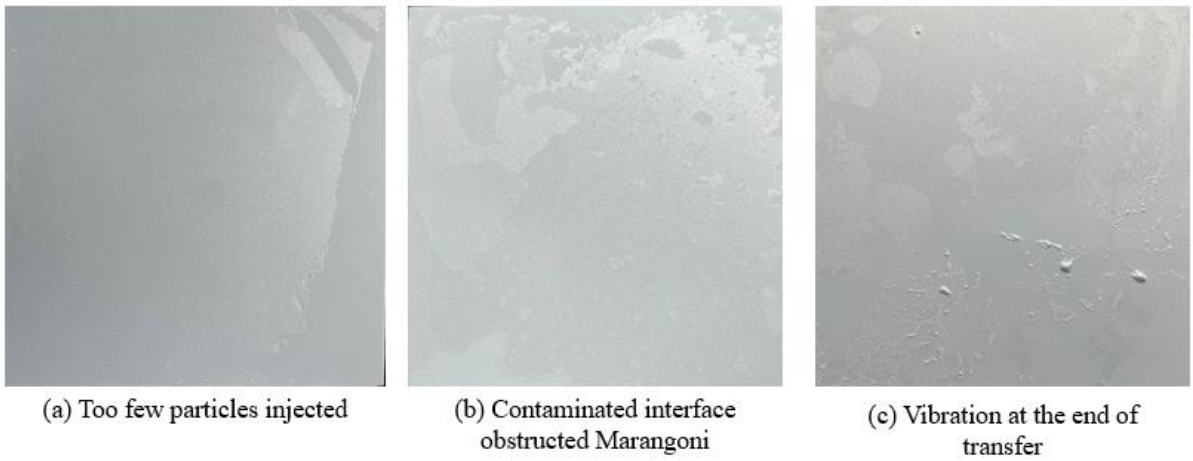

(a) Too few particles injected

(b) Contaminated interface obstructed Marangoni

(c) Vibration at the end of transfer

Figure 36: Images of incompletely coated substrates along with their suspected cause of for failure

Learning from the many failed initial attempts, the team was able to correct all problems and properly tune all required parameters. Once the machine was properly set up and all external disturbances were controlled for, high quality, fully coated substrates were produced, accomplishing the goal of this Capstone project. An image of a fully coated, 9in-by-9in substrate in hBN can be seen in Figure 37.

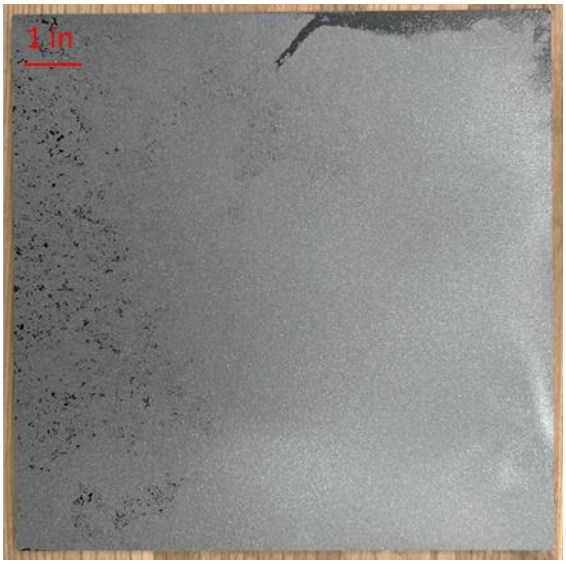

Figure 37: Image of 9in-by-9in fully coated substrate

The final step to confirm that the device made a high-quality monolayer was to view the microstructure under a microscope. A 20x magnification microscope image of the substrate shown in Figure 37 above is shown in Figure 38.

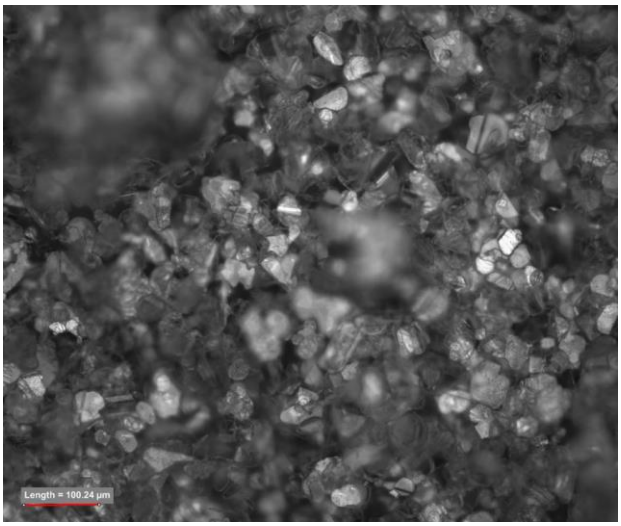

Figure 38: 20x microscopic image of hBN monolayer microstructure

The microstructure confirms that the monolayer is highly dense. The individual hexagonal shaped hBN particles can be seen touching one another in the image. This confirms that the monolayer is percolated which should correlate to a high thermal conductivity.

The final design was successful at fully coating a 9in-by-9in substrate in a percolated monolayer of hBN. A lot of testing had to be completed prior to obtaining a successful result but once all parameters and disturbances were controlled, the apparatus worked as desired.

4 Discussion and Conclusions

Even with a fully functional prototype that can coat a 9in-by-9in substrate in an hBN monolayer, there are many improvements that could be implemented to improve the user experience and the robustness of the design. The first improvement would be speeding up the process. Right now, it takes roughly 22 minutes for all three subsystems to work consecutively. Decreasing the run time would increase the throughput of the process, making it more economical. The easiest subsystem to speed up is injection. Adding additional pumps would make the injection faster while still limiting sedimentation in the trough. There could potentially be one pump in every corner of the trough to cut the injection time by a factor of four. Another aspect that could be sped up is the transfer. Currently, the transfer moves vertically at 1 mm/min and must travel a total distance of 20 mm. This means that the transfer takes roughly 20 minutes to complete. The

limits of the transfer speed were not tested during this Capstone project and the conservative 1 mm/min speed was used throughout. However, testing the maximum speed that transfer can occur at while still procuring high quality monolayers may enable the transfer speed to be increased, which would speed up the transfer process.

One more improvement would be to make the process more robust. This could be done in two ways. First by adding vibration dampening to the system and second by implementing closed loop control to the process. Reducing vibration with spring-mass dampeners would decrease the dependency of the prototype on the environmental conditions. This would enable it to be used in environments that are less closely controlled. Secondly, adding closed-loop control would relax some of the requirements of the user in tuning the system. Currently, the number of particles injected onto the air-water interface is estimated in an open-loop method with no feedback. If a pump or the magnetic stirrer malfunctions there is no way for the system to know that the incorrect number of particles was injected. Adding a sensor to the system that measured the number of particles injected via a surface tension probe would mean that closed-loop feedback and error detection could be added.

At the conclusion of this Capstone semester, the device was transferred to Northeastern's DAPS lab for researchers to use it to characterize and improve the electrical and thermal properties of the monolayer. The device allows researchers to easily create sample monolayers in an autonomous fashion, improving the throughput and the consistency of trials. The actual 9in-by-9in monolayers that were created by this Capstone team will undergo thermal testing in the DAPS lab and potential insertion testing at Kymeta to test the RF interference. If these tests show that a percolated hBN monolayer performs better than other materials, then hBN monolayers may be used by Kymeta to improve radome functionality.

5 References

[1] J.-C. Zheng *et al.*, "High thermal conductivity of hexagonal boron nitride laminates," *2D Mater.*, vol. 3, no. 1, p. 011004, Jan. 2016, doi: 10.1088/2053-1583/3/1/011004.

[2] Directed Assembly of Particles & Suspensions. *Marangoni with Langmuir-Blodgett Demonstration*, (Jul. 15, 2022).

[3] "surface tension | Definition, Examples, & Facts | Britannica." https://www.britannica.com/science/surface-tension (accessed Aug. 10, 2022).

[4] "Measuring Surface Tension of Water with a Penny | Science Project," *Science Buddies*. https://www.sciencebuddies.org/science-fair-projects/project-ideas/Chem_p021/chemistry/measuring-surface-tension-of-water-with-a-penny (accessed Aug. 10, 2022).

[5] "What is the Difference Between Surface Tension and Surface Energy." https://www.brighton-science.com/blog/what-is-the-difference-between-surface-tension-and-surface-energy-1 (accessed Nov. 11, 2022).

[6] "What is wettability?" https://www.biolinscientific.com/blog/what-is-wettability (accessed Aug. 11, 2022).

[7] "Surface Wettability | Institute of Interfacial Process Engineering and Plasma Technology | University of Stuttgart." https://www.igvp.uni-stuttgart.de/en/research/plasma-technology/processes/surface-wettability/ (accessed Aug. 11, 2022).

[8] A. Ranowsky, "Contact Angle and Surface Tension - A Fascinating Liaison." https://www.cscscientific.com/csc-scientific-blog/how-does-contact-angle-relate-to-surface-tension (accessed Nov. 11, 2022).

[9] R. Sharma *et al.*, "Autophobing on Liquid Subphases Driven by the Interfacial Transport of Amphiphilic Molecules," *Langmuir*, vol. 28, no. 43, pp. 15212–15221, Oct. 2012, doi: 10.1021/la303639w.

[10] "Contact Angle Goniometer | Low Price Measurement | Ossila." https://www.ossila.com/en-us/products/contact-angle-goniometer (accessed Nov. 11, 2022).

[11] R. Gengler, "A modified Langmuir Schaefer method for the creation of functional thin films," University of Groningen, Groningen, 2010. Accessed: Aug. 08, 2022. [Online]. Available: https://research.rug.nl/en/publications/a-modified-langmuir-schaefer-method-for-the-creation-of-functiona

[12] "Sedimentation." https://water.mecc.edu/exam_prep/SedimentationBasins.htm (accessed Aug. 13, 2022).

[13] "Sonication: Definition, Working Principle, Applications & Methods." https://byjus.com/physics/sonication/ (accessed Aug. 13, 2022).

[14] "Sonicators | Fisher Scientific." https://www.fishersci.com/us/en/browse/90180023/sonicators?page=1 (accessed Aug. 15, 2022).

[15] "Stirrer - Magnetic Stirring | Stirring and Mixing | Technical information | BOLA - Tubing, Stirrer Shafts, Magnetic Stirring Bars - Labware made of PTFE." https://www.bola.de/en/technical-information/stirring-and-mixing/stirrer-magnetic-stirring/ (accessed Aug. 13, 2022).

[16] "Stokes' Law." https://galileo.phys.virginia.edu/classes/152.mf1i.spring02/Stokes_Law.htm (accessed Oct. 20, 2022).

[17] "Why Ethanol is Soluble in Water - Solubility Property." https://byjus.com/jee-questions/why-ethanol-is-soluble-in-water/ (accessed Aug. 14, 2022).

[18] X. Lin, G. Fang, Y. Liu, Y. He, L. Wang, and B. Dong, "Marangoni Effect-Driven Transfer and Compression at Three-Phase Interfaces for Highly Reproducible Nanoparticle Monolayers," *J. Phys. Chem. Lett.*, vol. 11, no. 9, pp. 3573–3581, May 2020, doi: 10.1021/acs.jpclett.0c01116.

[19] C. Xie *et al.*, “Marangoni Force Assisted Spreading and Printing of Nanometer-Thick Polymer Films for Ubiquitous Optoelectronic Devices,” *Adv. Mater. Technol.*, vol. 6, no. 7, p. 2100181, 2021, doi: 10.1002/admt.202100181.
[20] Directed Assembly of Particles & Suspensions. *Scale up of a thermal coating monolayer technique*, (Jul. 05, 2022).
[21] “Langmuir Films,” *Nanoscience Instruments*. https://www.nanoscience.com/techniques/langmuir-films/ (accessed Aug. 05, 2022).
[22] X. Li and J. F. Gilchrist, “Large-Area Nanoparticle Films by Continuous Automated Langmuir–Blodgett Assembly and Deposition,” *Langmuir*, vol. 32, no. 5, pp. 1220–1226, Feb. 2016, doi: 10.1021/acs.langmuir.5b03760.
[23] M. Rojewska, M. Skrzypiec, and K. Prochaska, “The wetting properties of Langmuir–Blodgett and Langmuir–Schaefer films formed by DPPC and POSS compounds,” *Chem. Phys. Lipids*, vol. 221, pp. 158–166, Jul. 2019, doi: 10.1016/j.chemphyslip.2019.04.004.
[24] “free energy | Definition, Units, Gibbs, Helmholtz, Symbol, Equation, & Facts | Britannica.” https://www.britannica.com/science/free-energy (accessed Oct. 19, 2022).
[25] “KSV NIMA Langmuir Trough,” *Nanoscience Instruments*. https://www.nanoscience.com/products/langmuir-blodgett-troughs/ksv-nima-langmuir-trough/ (accessed Aug. 08, 2022).
[26] “Langmuir & Langmuir-Blodgett Troughs | Fabrication & deposition of thin films.” https://www.biolinscientific.com/ksvnima/fabrication-and-deposition-of-thin-films/langmuir-and-langmuir-blodgett-troughs (accessed Aug. 05, 2022).
[27] “Langmuir-Blodgett Troughs - Nanoscience Instruments.” https://www.nanoscience.com/products/langmuir-blodgett-troughs/ (accessed Jul. 19, 2022).
[28] G. Wills, “Your Recent KSV NIMA Roll-to-Roll LB Inquiry,” Jul. 25, 2022.
[29] “Magnetic Stirrer 4.72 Inch Stir Plate Magnetic Mixer 2500 RPM Speed Stirrer Machine with 4 Stir Bars for Milk Tea Coffee Wine Laboratory Liquid Stirring: Amazon.com: Industrial & Scientific.” https://www.amazon.com/Magnetic-Stirrer-Machine-Laboratory-Stirring/dp/B09FKWGJ66/ (accessed Nov. 18, 2022).
[30] “Erlenmeyer Flasks | Fisher Scientific.” https://www.fishersci.ca/ca/en/browse/90111066/erlenmyer-flasks (accessed Nov. 18, 2022).
[31] “Peristaltic Pumps Technology | Thomas Pumps.” https://www.gardnerdenver.com/en-us/thomas/knowledge-hub/peristaltic-pump (accessed Oct. 21, 2022).
[32] “Formlabs Form 3 SLA 3D Printer.” https://sourcegraphics.com/3d/printers/formlabs/formlabs-form-3/ (accessed Nov. 23, 2022).
[33] Caunter, Andrew, “Design Review,” Sep. 27, 2022.
[34] A. Kumar Verma and A. Govind Rajan, “Surface Roughness Explains the Observed Water Contact Angle and Slip Length on 2D Hexagonal Boron Nitride,” *Langmuir*, vol. 38, no. 30, pp. 9210–9220, Aug. 2022, doi: 10.1021/acs.langmuir.2c00972.
[35] J. A. Spink, “The transfer ratio of Langmuir-Blodgett monolayers for various solids,” *J. Colloid Interface Sci.*, vol. 23, no. 1, pp. 9–26, Jan. 1967, doi: 10.1016/0021-9797(67)90080-X.